

# The Crystal Structures of $\text{Mn}(\text{ReO}_4)_2 \cdot 2\text{H}_2\text{O}$ and of the Anhydrous Perrhenates $M(\text{ReO}_4)_2$ of Divalent Manganese, Cobalt, Nickel, and Zinc

A. Butz, G. Miehe, H. Paulus, P. Strauss, and H. Fuess<sup>1</sup>

*Fachbereich Materialwissenschaft, Fachgebiet Strukturforchung, Technische Universität, Petersenstraße 23, D-64287 Darmstadt, Germany*

Received October 1, 1997; in revised form March 1, 1998; accepted March 1, 1998

**$\text{Mn}(\text{ReO}_4)_2 \cdot 2\text{H}_2\text{O}$  (manganese(II)-perrhenate dihydrate) is analyzed by X-ray single-crystal diffraction and TG/DTA. Space group  $C2/m$ ,  $a = 14.71(1)$  Å,  $b = 5.861(6)$  Å,  $c = 5.537(5)$  Å,  $\beta = 110.87(4)^\circ$ ,  $Z = 2$ , calculated density  $D_x = 4.40$  g/cm<sup>3</sup>. Chains of interconnected  $\text{ReO}_4$ -tetrahedra and  $\text{MnO}_4(\text{OH})_2$ -octahedra run parallel  $[010]$ . The AC-susceptibility ( $\mu_{\text{eff}} = 5.7\mu_B$ ) is consistent with divalent Mn and heptavalent Re. Dehydration takes place in a single step at 150°C. Decomposition starts at 820°C. The dehydration product  $\text{Mn}(\text{ReO}_4)_2$  and the isotypic anhydrous perrhenates of Co, Ni, Zn crystallize in space group  $P\bar{3}$ ,  $Z = 1$ ;  $a$  ranges from 5.67 (Ni) to 5.86 Å (Mn),  $c$  ranges from 6.07 (Mn) to 6.17 Å (Zn),  $D_x$  (g/cm<sup>3</sup>) = 5.11 (Mn), 5.36 (Co), 5.44 (Ni), 5.33 (Zn). The structure is topologically equivalent to that of  $\beta\text{-Zr}(\text{MoO}_4)_2$ .  $M^{2+}\text{O}_6$ -octahedra are linked by  $\text{ReO}_4$ -tetrahedra to form layers which are not interconnected.** © 1998 Academic Press

## INTRODUCTION

The crystal structures of the tetrahydrates of  $M(\text{ReO}_4)_2$ ,  $M = \text{Zn}$  and  $\text{Co}$  were previously reported by our group (1). The present communication deals with the crystal structures of the dihydrate  $\text{Mn}(\text{ReO}_4)_2 \cdot 2\text{H}_2\text{O}$  and of the anhydrous compounds  $M^{2+}(\text{ReO}_4)_2$ , where  $M = \text{Mn}, \text{Co}, \text{Ni}, \text{Zn}$ . The main feature of the perrhenates, the salts of the perrhenic acid  $\text{HReO}_4$ , is the tetrahedral  $[\text{ReO}_4]^-$  ion (2). Perrhenates of alkali, alkaline-earth, and transition metal cations have been reported in the literature early this century, but only a few crystal structures have been described. In 1980, Ovchinnikov *et al.* (3) prepared manganese perrhenate by reacting perrhenic acid with excess manganese carbonate at 60–80°C. The residue has been dehydrated in air at 120°C for 3 h. Only the thermal decomposition of the so-prepared compound has been investigated. Although a number of anhydrous perrhenates of divalent cations have been reported in the literature (4–9), structural information is

scarce. A first approach to crystal structure determination was performed by Varfolomeev *et al.* in 1983 (9). From X-ray powder diffraction data of  $\text{Mg}(\text{ReO}_4)_2$  these authors found similarities to the  $\text{Zr}(\text{MoO}_4)_2$ -type (10). In 1990, Varfolomeev *et al.* (11) published cell parameters for anhydrous nickel perrhenate which are close to those of  $\text{Zr}(\text{MoO}_4)_2$ .

## EXPERIMENTAL

The preparation of the perrhenate dihydrates was carried out in two steps (1). Dissolving 500-mg high-purity rhenium powder (99.995%, ALDRICH) in 20-ml 30% aqueous hydrogen peroxide (ALDRICH) yields a colorless solution of perrhenic acid,  $\text{HReO}_4$  (12). A 20% excess of  $\text{MnCO}_3$  (99.9+%, Aldrich) was added to a solution of freshly prepared perrhenic acid. The reaction starts at a temperature between 50 and 60°C under release of  $\text{CO}_2$  bubbles. At the end of the reaction the formation of  $\text{CO}_2$  bubbles stops. Then the excess carbonate was filtered off, and the solution was kept on a water bath (56°C) until a thin crystalline surface layer formed. The solution was then removed from the water bath and kept at room temperature.  $\text{Mn}(\text{ReO}_4)_2 \cdot 2\text{H}_2\text{O}$  crystals of different shape grew after 5–7 days.

The anhydrous perrhenates were obtained by heating the powdered di- or tetrahydrates in open crucibles. At temperatures ca. 90 K below the decomposition temperatures as determined by DTA/TG measurements (Mn, 820°C; Co, 871°C; Ni, 882°C; Zn, 734°C) dehydration was completed after 24 h. The colors of the hydrates (pale pink, blue, and green for Mn, Co, and Ni, respectively) intensify during dehydration. The Zn compounds are colorless. To avoid rehydration, the perrhenates were stored in sealed preparation tubes in an evacuated desiccator over  $\text{CaCl}_2$ .

Single-crystal data of the dihydrate were collected on a STOE-STADI-4 diffractometer with graphite monochromatized  $\text{MoK}\alpha$ -radiation and a scintillation counter.

<sup>1</sup>To whom correspondence should be addressed.

X-ray powder diffraction studies were performed on a STOE-STADI-P diffractometer using Ge(111)-monochromatized  $\text{CuK}\alpha_1$ -radiation and a linear PSD covering a  $2\theta$  range of  $4^\circ$ . The material was contained in a sealed glass capillary of 0.3 mm diameter.

The magnetic studies were carried out in a temperature range of 15 to 200 K using an AC-susceptometer (Lake Shore Cryotronics Model 7000).

Thermal analysis was performed with a DTA/TG-system (SETARAM DTG 92.16.18) in argon atmosphere.

## DETERMINATION, DESCRIPTION, AND DISCUSSION OF THE STRUCTURES

### 1. The Dihydrate $\text{Mn}(\text{ReO}_4)_2 \cdot 2\text{H}_2\text{O}$

**Structure Determination.** A  $0.10 \times 0.16 \times 0.15 \text{ mm}^3$  sized, prism-shaped, pale pink colored single crystal was chosen for structure determination. Initial lattice parameters were obtained by film methods and refined at the diffractometer from 22 reflections in the  $2\theta$  range  $27.0\text{--}33.9^\circ$ . Intensities of 834 reflections up to  $d_{\min} = 0.84 \text{ \AA}$  were recorded at room temperature within the half sphere  $k \geq 0$ . Standard reflections  $31\text{--}1$  and  $\text{--}311$  were measured every 4 h and showed consistency within 1%. A numerical correction for absorption was performed using the program SHELX-76 (13).

Out of 431 unique reflections, five weak reflections with extremely unbalanced background were rejected, the remaining were used for structure determination and refinement. The structure was solved using the Patterson routine of the program SHELXS-86 (14) and refined with SHELX-76 (13).

Table 1 lists the final cell parameters, agreement factors, and atomic parameters. The hydrogen atoms could not experimentally be determined. The interatomic distances and bond angles are given in Table 2.

**Description and Discussion.**  $\text{Mn}(\text{ReO}_4)_2 \cdot 2\text{H}_2\text{O}$  crystallizes in space group  $C2/m$  with two formula units per unit cell. The structure consists of  $\text{ReO}_4$ -tetrahedra and  $\text{MnO}_6$ -octahedra, which build up chains along  $[010]$ . A plot of the structure is given in Fig. 1 (a polyhedral plot in Fig. 4b). Within the chains, O(3) is bound merely to Mn. Because perrhenium acid is a strong acid, it is expected that hydrogen atoms are not attached to the oxygen atoms of  $\text{ReO}_4$ -tetrahedra. Therefore O(3) must be the oxygen of the water molecule. The distances between O(3) and the atoms O(4) and O(2) of the neighboring chains are 2.75 and 2.91 Å, respectively (Table 2). This is within the range of hydrogen bonds of medium strength.

The tetrahedral coordination of rhenium is slightly distorted. The Re–O distances within the tetrahedron are between 1.73 and 1.77 Å, the O–Re–O-angles range from  $95.4$  to  $112.9^\circ$ . The mean Re–O distance of 1.76 Å corresponds to

**TABLE 1**  
 **$\text{Mn}(\text{ReO}_4)_2 \cdot 2\text{H}_2\text{O}$ : Cell Parameters, Agreement Factors, Atomic Parameters, and Anisotropic Temperature Coefficients**

Space group	$a$ (Å)	$b$ (Å)	$c$ (Å)	$\beta$ ( $^\circ$ )	$V$ (Å <sup>3</sup> )	$R(F)$	$R_w(F)$
$C12/m1$	14.710(11)	5.861(6)	5.537(5)	110.87(4)	446.1(11)	0.087	0.079

Atom	Wyck. pos.	$x$	$y$	$z$
Re	4i	0.6338(1)	0	0.3492(4)
Mn	2c	0	0	1/2
O(1)	8j	0.5653(2)	0.7578(4)	0.3415(5)
O(2)	4i	0.7459(3)	0	0.6128(8)
O(3)	4i	0.8780(2)	0	0.1511(7)
O(4)	4i	0.6858(5)	0	0.1079(7)

Atom	$u_{11}$	$u_{22}$	$u_{33}$	$u_{12}$	$u_{13}$	$u_{23}$
Re	0.028(1)	0.024(1)	0.028(1)	0	0.008(1)	0
Mn	0.048(7)	0.034(6)	0.032(6)	0	0.005(3)	0
O(1)	0.059(2)	0.040(2)	0.075(2)	$-0.027(2)$	0.022(3)	0.005(2)
O(2)	0.045(3)	0.093(4)	0.07(3)	0	0.006(3)	0
O(3)	0.008(3)	0.070(3)	0.056(2)	0	0.001(2)	0
O(4)	0.129(5)	0.043(3)	0.146(5)	0	0.109(4)	0

values for other perrhenates with Re in tetrahedral coordination (15, 16) and to the sum of the effective ionic radii (17, 18). The O–O distances representing the edges of the tetrahedron are between 2.61 and 2.91 Å.

Manganese is coordinated by a fairly regular octahedron of oxygen atoms. The two axial oxygen atoms [O(3),  $\text{H}_2\text{O}$ -molecules] are 2.12 Å distant from the central ion. They are the donors of the hydrogen-bridges to the  $\text{ReO}_4$  ions of neighboring chains. The distance to the equatorial oxygen atoms [O(1)] is 2.14 Å. Mn–O (–Re)– distances are slightly larger than those of Mn–OH<sub>2</sub>. This is a consequence of the

**TABLE 2**  
 **$\text{Mn}(\text{ReO}_4)_2 \cdot 2\text{H}_2\text{O}$ : Interatomic Distances (Å) and Bond Angles ( $^\circ$ )**

Atoms	Distance (Å)	Atoms	Bond angle ( $^\circ$ )
Re–O(1)	1.73(3)	(2 $\times$ ) O(1)–Re–O(1)	110.1(2)
Re–O(2)	1.77(5)	O(1)–Re–O(2)	112.5(1)
Re–O(4)	1.76(4)	O(1)–Re–O(4)	112.9(1)
Mn–O(1)	2.14(2)	O(2)–Re–O(4)	95.4(2)
Mn–O(3)	2.12(3)	(2 $\times$ ) O(1)–Mn–O(1)	90.1(2)
Mn–Re	3.78(3)	O(3)–Mn–O(1)	89.1(1)
Re–Re	4.36(3)		
O(3)–O(4)	2.75 <sup>a</sup>		
O(3)–O(2)	2.91 <sup>a</sup>	Mn–O(1)–Re	155.6(2)

<sup>a</sup> Possible hydrogen bond.

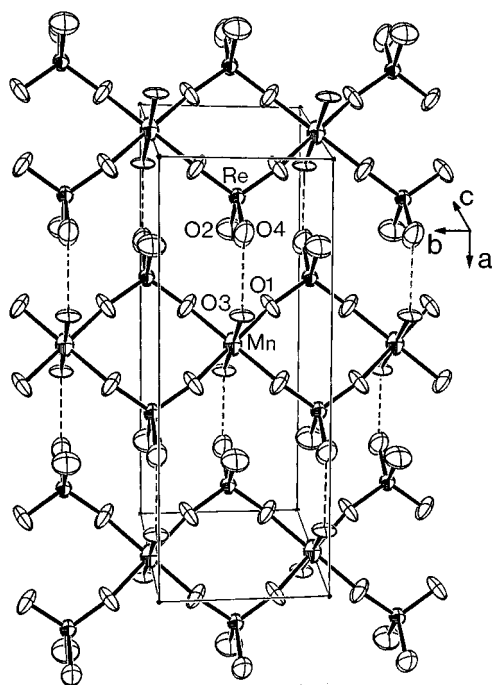


FIG. 1.  $\text{Mn}(\text{ReO}_4)_2 \cdot 2\text{H}_2\text{O}$ . a, View parallel [001], horizontal,  $b$ -axis, probability ellipsoids 50%; broken lines, OH bridges.

polarizing effect of the sevenfold charged rhenium ions (19). The O–O edges of the octahedron are 2.98 and 3.03 Å.

**Magnetic Susceptibility.** From the minimum accessible temperature of 15 K up to 200 K,  $\text{Mn}(\text{ReO}_4)_2 \cdot 2\text{H}_2\text{O}$  exhibits paramagnetic Curie–Weiss behavior. The values derived by fitting the data from temperatures below 100 K are:  $\theta = -3(1)\text{K}$  and  $\mu_{\text{eff}} = 5.7(3)\mu_{\text{B}}$ . This value is consistent with the theoretical value  $\mu_{\text{eff}} = 5.9\mu_{\text{B}}$  for  $\text{Mn}^{2+}$ .

**Thermal Analysis.** Manganese perrhenate dihydrate exhibits a single dehydration step at 150°C. A single step is expected because the four water molecules per cell are symmetrically equivalent. No phase transition has been detected between dehydration and the melting point at 820°C.

Thermal decomposition starts at 820°C and leads to gaseous rhenium(VII)-oxide and manganese(II)-oxide, which has been identified to be the only nonvolatile residue (3).

## 2. The Anhydrous Perrhenates $M^{2+}(\text{ReO}_4)_2$ ( $M = \text{Mn}, \text{Co}, \text{Ni}, \text{Zn}$ )

**Structure Determination.** Because no suitable crystals are available, X-ray powder data of the Mn compound recorded up to  $d_{\text{min}} = 1.14\text{Å}$  were used for an *ab initio* structure determination by Patterson methods. The hexagonal metrics of the cell (Table 3) enforce the use of Patterson group  $P6/mmm$  during the initial steps of structure

TABLE 3  
 $M^{2+}(\text{ReO}_4)_2$ : Cell Parameters and Reliability Factors of the Rietveld Refinements

$M^{2+}$	Mn	Co	Ni	Zn
Color	pink	blue	green	—
$P\bar{3}$				
$a$ (Å)	5.8579(1)	5.7229(2)	5.6669(1)	5.7419(2)
$c$ (Å)	6.0665(2)	6.1111(2)	6.1357(1)	6.1696(3)
$a/c$	0.9656	0.9364	0.9236	0.9307
$V$ (Å <sup>3</sup> )	180.31	173.34	170.65	176.15
Rp (%)	7.91	4.61	8.36	9.69
Rwp (%)	10.57	6.35	11.46	12.83
Rb (%)	6.30	2.93	5.94	3.09
GOF	1.02	2.93	1.11	2.18

determination. Derived from the diffractogram were 23  $|F_{hkl}|^2$  values. Together with the absence of systematic extinctions, the features of the three-dimensional Patterson function lead to  $P\bar{3}2/m1$  as the space group of highest-possible symmetry. Despite the discrepancy between the true and the assumed Laue group, the positions of the Mn and Re atoms could immediately be determined. Positions of the O atoms were derived from crystal chemical considerations. They coincide with peaks in the difference Fourier map after a first Rietveld refinement (20) of the Mn and Re atoms in space group  $P\bar{3}2/m1$ . Because of short Mn–O distances after refinement of the complete structure, the  $x$  and  $y$  parameters of O(1) at  $x, 2x, z$  were untied. This means a symmetry reduction to  $P\bar{3}$ . The refinement in this space group leads to reasonable interatomic distances and angles. Cell parameters from Rietveld refinement and reliability factors are given in Table 3; atomic coordinates are given in Table 4 (left side). Figure 2 gives the observed and calculated diffractograms and the residuals. The features in the difference curve are mainly caused by the  $hkl$ -dependence of the line width as a result of strong anisotropy of crystal shape.

After determination of the structure, we realized a great similarity with the high-temperature form of  $\text{Zr}(\text{MoO}_4)_2$  which has been determined from single-crystal data by Auray *et al.* (10): space group  $P\bar{3}12/c$ ,  $a = 10.139\text{Å}$ ,  $c = 11.708\text{Å}$ . This cell is obtained from the  $M^{2+}(\text{ReO}_4)_2$  cell by the transformation matrix (2,1,0; -1,1,0; 0,0,2). By means of selected area electron diffraction, it is, however, assured that in  $M^{2+}(\text{ReO}_4)_2$  no supercell is present, at least under the conditions inside an electron microscope.

A powder diffractogram calculated with the structural parameters of  $\text{Zr}(\text{MoO}_4)_2$  but Zr and Mo replaced by Mn and Re, respectively, shows that all additional reflections originating from the increase of the cell volume by a factor of 6 (i.e., reflections not belonging to the two parity groups

TABLE 4  
Atomic Coordinates for  $M^{2+}(\text{ReO}_4)_2$  Compared with the Transformed Coordinates for  $\text{Zr}(\text{MoO}_4)_2$

		$M^{2+}(\text{ReO}_4)_2$				$\text{Zr}(\text{MoO}_4)_2$ , transformed				
Atom	$M^{2+}$	$x$	$y$	$z$	$D$	Atom	$x$	$y$	$z$	$D$
$M^{2+}$		0	0	0		Zr(1)	0	0	0	
(1a)						Zr(2)	0	0	-0.01868	
Re	Mn	1/3	2/3	0.2891(4)		Mo	0.31851	0.66762	0.29800	
(2d)	Co			0.2805(6)						
	Ni			0.2799(3)						
	Zn			0.2819(7)						
O(1)	Mn	0.135(5)	0.349(3)	0.206(4)	0.128	O(1)	0.1798	0.3395	0.2016	-0.029
(6g)	Co	0.143(6)	0.343(3)	0.191(3)	0.091	O(2)	0.1687	0.3405	0.1628	0.005
	Ni	0.120(2)	0.325(2)	0.186(2)	0.150	O(3)	0.1749	0.3406	0.2356	-0.013
	Zn	0.148(10)	0.347(4)	0.177(3)	0.079	Mean	0.1745	0.3402	0.2000	-0.013
O(2)	Mn	1/3	2/3	0.570(7)		O(4)	0.2856	0.6711	0.5846	
(2d)	Co			0.602(4)						
	Ni			0.602(2)						
	Zn			0.542(7)						

$D = (y - 2x)/(y + 2x)$ , a measure of the deviation from  $P\bar{3}2/m1$ .

$h - k = 3n$  and  $l = 2n$ ) are very weak. Model calculations suggest that the strongest supercell lines of the  $\text{Zr}(\text{MoO}_4)_2$  structure type (021, 121, 131,  $23\bar{1}$ ) should exceed the level of noise in the diffractograms; no indications, however, were found (Fig. 2).

*Description and Discussion.* The structure of  $M^{2+}(\text{ReO}_4)_2$  is built from layers which are stacked in  $[001]$ -direction, the distance of two layers being  $c$ . Although partially

distinguished by different hatching in Fig. 3, all octahedra as well as all tetrahedra are symmetrically equivalent. Figure 4c gives a projection down  $c$ . The layers consist of  $M^{2+}\text{O}_6$ -octahedra linked by  $\text{ReO}_4$ -tetrahedra. Within a layer, the linking atoms O(1) form two Kagomé nets, whereas the apical atom O(2) of the  $\text{ReO}_4$  tetrahedron is bound to Re only. The closest contact between two layers is formed by O(1)-O(2) distances of ca. 3.0 Å. Some interatomic distances and angles are given in Table 5. The cell

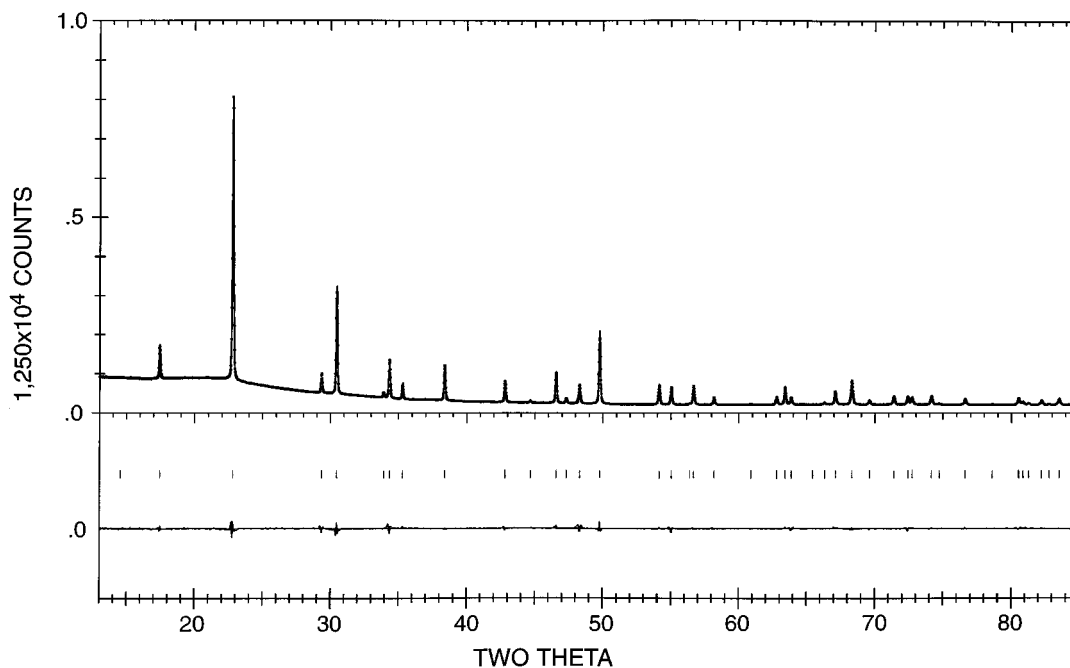


FIG. 2.  $\text{Mn}(\text{ReO}_4)_2$ . Observed and calculated diffractograms and difference plot ( $\text{CuK}\alpha_1$ ).

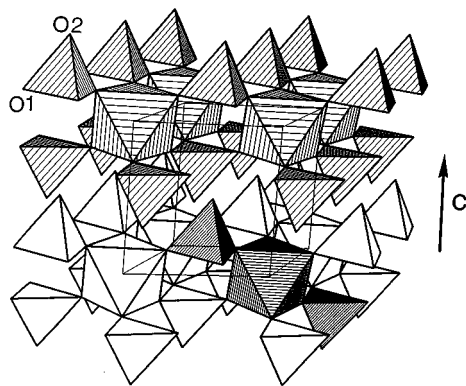


FIG. 3. Polyhedral plot of  $M^{2+}(\text{ReO}_4)_2$ . Octahedra,  $\text{MnO}_6$ ; tetrahedra,  $\text{ReO}_4$ . The two layers are translationally equivalent. A  $[M^{2+}\text{Re}_2\text{O}_{12}]^{8-}$  group is distinguished by dense hatching.

volumes (Table 3) follow the trend of the ionic radii of six-coordinated  $M^{2+}$ .

Table 4 compares the structural parameters of the four perrhenates with the parameters for  $\text{Zr}(\text{MoO}_4)_2$ , transformed to the  $M^{2+}(\text{ReO}_4)_2$  cell. In the perrhenates, the aristotype structure is distorted by a twisting of octahedra and tetrahedra; the axis of rotation is parallel  $c$ . This is expressed by a distinct deviation of O(1) from the site  $x$ ,  $2x$ ,  $z$ . The distortions in the molybdate structure are different. Here mainly the tetrahedra are tilted with respect to the aristotype structure. The tilt axes are predominantly perpendicular to  $c$ . This leads to a strong variation of the  $z$  parameter of the transformed atoms O(1) to O(3) and to a shift of the transformed O(4) from the threefold axis.

Layers of the  $M(\text{ReO}_4)_2$  type are very common in phosphates, sulfates, and silicates. The topological aspects of the involvement of such layers in sulfate and silicate structures are discussed by Moore (21). A prototype structure is that of glaserite  $[\text{K}_3\text{Na}(\text{SO}_4)_2]$ ,  $P\bar{3}2/m$ ,  $a = 5.66 \text{ \AA}$ ,  $c = 8.00 \text{ \AA}$ ,  $Z = 1$ , e.g., Ref. 21]. Here the  $\text{Na}^+(\text{SO}_4)_2$ -layers are connected by  $\text{K}^+$  at  $0,0,1/2$ , and position  $1/3,2/3,z$  is occupied in addition. In the dehydrated alum  $\text{KAl}(\text{SO}_4)_2$  ( $P\bar{3}$ ,  $a = 4.71 \text{ \AA}$ ,  $c = 8.00 \text{ \AA}$ ,  $Z = 1$ ) which has recently been reinvestigated (22), the  $\text{Al}^{3+}(\text{SO}_4)_2$ -layers are connected by  $\text{K}^+$  at  $0,0,1/2$ , whereas the position  $1/3,2/3,z$  remains empty.

An outstanding feature in the anhydrous perrhenates is the contact between the  $A(\text{BO}_4)_2$  layers which is not obtained by additional cations. The oxygen atoms, which are bonded to the tetrahedrally coordinated  $B$  cation only [O(2) in Table 4, left side] are distinguished by a large atomic displacement factor and a short B–O distance in many compounds containing those layers. This feature is discussed by Auray *et al.* (10). The comparatively long O(2)– $M^{2+}$  distances found for  $M^{2+} = \text{Co}$  and  $\text{Ni}$  might be the result of limited accuracy of the data: Atom O(2) is one of four independent atoms, but it represents only ca. 6.5% of

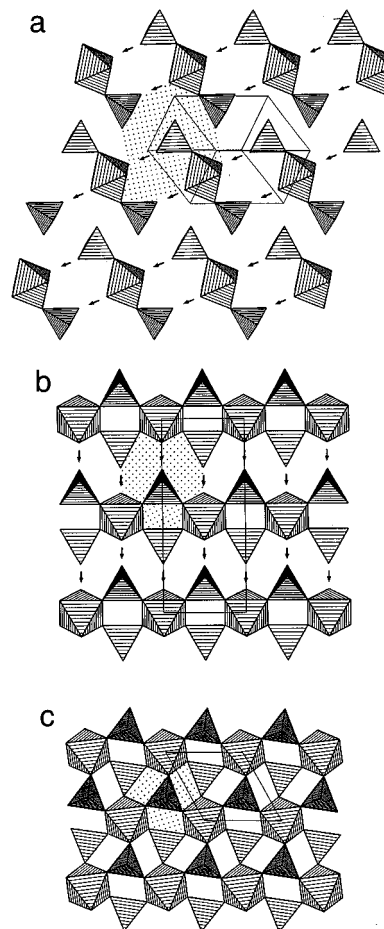


FIG. 4.  $\text{Mn}(\text{ReO}_4)_2 \cdot n\text{H}_2\text{O}$ ,  $n = 4$ (a),  $2$ (b),  $0$ (c); the changing connectivity as dehydration proceeds is figured by the change in shape and connectivity of the stippled areas.

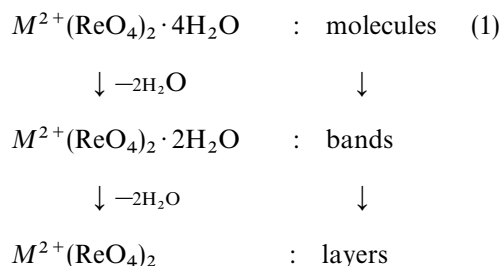
the scattering power. Hence the site parameter  $z$  of this atom and the Re–O(2) distance is not very reliable when determined from powder data. In addition, a slight preferred orientation with  $[001]$  as the direction of preference might have falsified particularly the  $z$  parameters, though a preferred orientation parameter has been refined.

TABLE 5  
Interatomic Distances and Angles for  $M^{2+}(\text{ReO}_4)_2$

$M^{2+}$	Mn	Co	Ni	Zn
$M^{2+}$ –O(1) ( $6 \times$ )	2.18(2)	2.07(2)	1.97(1)	2.05(3)
Re–O(1) ( $3 \times$ )	1.71(3)	1.70(3)	1.79(2)	1.72(4)
Re–O(2) ( $1 \times$ )	1.70(5)	1.97(4)	1.98(2)	1.60(5)
O(1)– $M^{2+}$ –O(1)	89.6(3)	88.7(3)	90.0(2)	85.8(5)
O(1)–Re–O(1)	111.6(6)	110.2(6)	110.2(4)	106.8(8)
O(1)–Re–O(2)	107.2(5)	108.7(5)	108.8(3)	112.1(6)

STRUCTURAL RELATIONS BETWEEN TETRAHYDRATE,  
DIHYDRATE, AND ANHYDROUS  $M^{2+}(\text{ReO}_4)_2$ 

The dehydration process



can be understood as a condensation of  $[M^{2+}\text{Re}_2\text{O}_{12}]^{8-}$  groups. The geometric relationship between the three structures is suggested in Fig. 4. As dehydration proceeds, the sites of the expelled water molecules which belong to the coordination octahedron of  $M^{2+}$  are replaced by O atoms of neighboring  $\text{ReO}_4$ -tetrahedra as indicated by the arrows in Fig. 4.

For  $M^{2+} = \text{Co}$ , there are indications from the TG/DTA data that within a small temperature range between the tetra- and the dihydrate a trihydrate is formed. Figure 4 suggests that a trihydrate should be built from molecules  $M_2^{2+}(\text{ReO}_4)_4 \cdot 6\text{H}_2\text{O}$ .

## ACKNOWLEDGMENTS

This work was supported by the Fonds der Chemischen Industrie. Thanks are due to the H. Starck GmbH, Goslar, for support with rhenium oxides.

## REFERENCES

1. A. Butz, I. Svoboda, H. Paulus, and H. Fuess, *J. Solid State Chem.* **115**, 255 (1995).
2. H. H. Claassen and A. J. Zielen, *J. Chem. Phys.* **22**, 707 (1954).
3. K. V. Ovchinnikov, E. N. Nikolaev, and G. A. Semenov, *J. Gen. Chem. USSR* **50**, 379 (1980). [Translated from *Zhurnal Obshchei Khimii* **50**, 485 (1980)]
4. W. T. Smith and G. E. Maxwell, *J. Amer. Chem. Soc.* **73**, 658 (1951).
5. L. L. Zaitseva, A. V. Velichko, A. A. Kruglov, and V. A. Zoto, *Russ. J. Inorg. Chem.* **23**, 2396 (1978). [Engl. Transl.]
6. L. L. Zaitseva, A. V. Velichko, and V. A. Zotov, *Russ. J. Inorg. Chem.* **23**, 1318 (1978). [Engl. Transl.]
7. L. L. Zaitseva, A. V. Velichko, A. V. Demin, A. I. Sukhikh, and N. V. Morgunova, *Russ. J. Inorg. Chem.* **27**, 357 (1982). [Engl. Transl.]
8. E. Wilke-Dörfurt and Th. Gunzert, *Z. Anorg. Allg. Chem.* **215**, 369 (1933).
9. M. Varfolomeev and N. B. Shamari, *Russ. J. Inorg. Chem.* **27**, 1216 (1983). [Engl. Transl.]
10. M. Auray, M. Quarton, and P. Tarte, *Acta Cryst.* **C42**, 257 (1986).
11. M. Varfolomeev, N. B. Shamari, H. I. Lunk, and T. N. Orlova, *Russ. J. Inorg. Chem.* **35**, 545 (1990). [Engl. Transl.]
12. R. D. Peacock, "Rhenium," *Comprehensive Inorganic Chemistry*, Vol. 3, Pergamon Press, Oxford/New York, 1973.
13. G. M. Sheldrick, SHELX-76, Program System for Crystal Structure Determination. University of Cambridge, 1976.
14. G. M. Sheldrick, SHELX-86, Program for the Solution of Crystal Structures. University of Goettingen, 1986.
15. J. F. Lotspeich, A. Javan, and A. Engelbrecht, *J. Chem. Phys.* **31**, 633 (1959).
16. T. Betz and R. Hoppe, *Z. Allg. Chem.* **500**, 23 (1993).
17. R. D. Shannon and C. T. Prewitt, *Acta Cryst.* **B25**, 925 (1969).
18. R. D. Shannon, *Acta Cryst.* **A32**, 751 (1976).
19. R. G. Matleeva, M. B. Varfolomeev, N. B. Samraj, and H. J. Lunk, *Z. Anorg. Allg. Chem.* **532**, 193 (1986).
20. D. B. Wiles and R. A. Young, Program LHPM 7, *J. Appl. Cryst.* **14**, 149 (1981) and C. J. Howard, R. J. Hill, AAEC report no. M112 (1986).
21. P. B. Moore, *Am. Mineral.* **58**, 32 (1973).
22. C. Pophal, "Diplomarbeit," Fachbereich Chemie, TH Darmstadt, 1994.